

Revisiting Protodyakonov's Pressure Arch Theory

Yong ZHU ^{a,1}, Hui ZHOU ^a, Chuanqing ZHANG ^a, Jun DONG ^b, Yuanzhou CHEN^b, Jun XIE ^b, Tianbing Xiang ^c and Xiaolong Yang ^c

^a State Key Laboratory of Geomechanics and Geotechnical Engineering, Institute of Rock and Soil Mechanics, Chinese Academy of Sciences, Wuhan, Hubei 430071, China

^b China Railway Siyuan Survey and Design Group CO., LTD, Wuhan, Hubei 430063, China

^c Kunming Engineering Corporation Limited. Kunming, Yunnan 650051, China

Abstract. Protodyakonov's pressure arch theory (PPAT) has been widely used in rock engineering design owing to its conciseness and clear engineering concept. However, the applicability of this theory to soil formations has not yet reached a consensus, mainly because of the lack of criterion for stable arching in soil and the fact that soil has a much lower strength than rocks. To fill this gap, the PPAT based on arch assumptions and arch stability requirements is revisited in this paper. A modified arch equation (M-PPAT) is established considering the lateral stress and arch foot resistance. Expressions for the arch strength and arch foot stability criteria are given. A trapdoor test and PFC2D simulation is conducted to verify the M-PPAT. The difference between the arch height calculated by M-PPAT and the trapdoor test result is only 3.3%, which is much better than the height given by PPAT. The particle flow simulation results for the trapdoor test by PFC2D show that the particle material can form a stable naturally balanced arch (NBA), and the shape of the arch is very close to the test results. Taking typical rock and soil formations as examples, the inferences obtained by M-PPAT are discussed. The arch foot stability criterion was used to test the stability of the arches formed in the soil using the arch axis equation, which does not consider the arch foot stability, and it was found that these arches are unstable except for M-PPAT. The arch height of stable NBA is limited by the arch foot stability criterion, and the maximum buried depth for stable NBA was found to be limited by the arch strength criterion. Since M-PPAT does not consider cohesion, this theory should be used with caution in cohesive soil formations. The research results can be used to determine the applicable scope of the surrounding earth pressure calculation method that is based on the PPAT. Moreover, they have reference value for designing underground space structures.

Keywords. Soil arch, arching criterion, surrounding earth pressure, arch strength criterion, arch foot stability criterion

1. Introduction

Proposed by the Soviet mining expert Protodyakonov in the 1930s, the pressure arch theory is a classical approach for evaluating rock loads acting on tunnels. It was

¹ Yong ZHU, Corresponding author, State Key Laboratory of Geomechanics and Geotechnical Engineering, Institute of Rock and Soil Mechanics, Chinese Academy of Sciences, Wuhan, Hubei 430071, China; E-mail: yzhu@whrsm.ac.cn

established based on the following facts: The excavation of an underground cave leads to stress redistribution in the surrounding rock, ultimately leading to the formation of a naturally balanced arch (NBA). The surrounding rock load on a tunnel structure is mainly the gravity of the loosening rock or soil below the arch. This theory has been widely used in rock engineering design owing to its conciseness and clear engineering concept, although the arch height in the codes [1-3] is determined using an empirical formula rather than an arch equation [4-6]. In view of the advances made using this theory in the design of mountain tunnels, urban underground space designers want to know whether this theory could be applied to soil formations. A challenging issue in the application of the classical arch theory to soil formations is that the strength of soil is much lower than that of rocks, which may prevent the formation of a stable NBA.

Although the arch effect is extensively employed in geotechnical engineering [7] and has received considerable attention [8-11], studies on the stability of the NBA are lacking. Hall et al. [12] proved that dilatancy and cohesiveness are the two conditions required for the stability of a sand arch around a wellbore. Guo et al. [13] derived the critical width of a stable arch made of a cohesionless material and the inclination angle at its foot relative to the horizontal by conducting trapdoor tests and stress-free surface analyses. Xu et al. [14] discussed the arching capacity of Shanghai clay by performing a series of centrifugal model tests. The authors concluded that arching cannot be done while tunneling in clay strata with an excessively shallow depth. Liang et al. [15,16] analyzed the influence of lithology and horizontal stress on the position and shape of the arch. The authors believed that the horizontal stress can provide sufficient support for the stability of the arch foot. Wang et al. [17] deduced the relationship between the bearing capacity of a rock arch structure and the horizontal reaction force. Jia et al. [18] studied the stress release characteristics of sand arches through model tests and numerical simulations. Based on the double-shear strength theory, Li et al. [19] determined the minimum buried depth of a natural arch of a soil tunnel. Niu et al. [20] outlined the necessary conditions for a stable arch: (1) There should be a "self-bearing structure" with a load transfer mechanism to maintain the stability of the surrounding rock; (2) The stable arch materials should meet the strength requirement; (3) The surrounding rock of the arch foot can provide sufficient support. Yang et al. [21] studied the influence of the lateral pressure coefficient on arching. Zheng et al. [22] proved through model tests and numerical simulations that if the strength of the surrounding rock material is too low, a stable NBA cannot be formed. Zhang et al. [23] established a composite tunnel surrounding rock structure model based on the arch theory and proposed a displacement criterion for judging the stability of arch structures. From the above research, the stability of soil arches is mainly related to the buried depth, cave span, soil parameters, lateral pressure coefficient, and other factors. The requirements for a stable arch formation in a rock mass have been put forward. However, the arching criterion is too complicated for engineering practice. Criteria for judging the stability of an NBA in soil formations are still required. A problem similar to the arch stability is the surrounding rock stability, whose representative criteria are the safety factor criterion based on the strength reduction method [24-26], displacement criterion based on theoretical derivation [26,27], empirical criteria based on field monitoring and numerical simulation [28,29], reliability criteria based on probability theory [30], and other comprehensive evaluation methods [31-33]. The self-stabilization span and time of an underground cave obtained on the basis of various rock mass quality classification standards [34,35] are derived from engineering

experience. The research results can be used as references for arch stability analyses, but cannot be directly used for judging the arch stability.

This study mainly improves the PPAT and establishes a stability criterion for NBA. An improved arch equation named M-PPAT is established considering the lateral stress and arch foot stability. Expressions for the arch strength criterion and arch foot stability criterion are given. A trapdoor experiment combined with a PFC2D numerical simulation is performed to verify the M-PPAT. Finally, typical rock and soil formation cases are taken as examples to show some interesting inferences and applicability of M-PPAT. The research results can be used to determine the applicable scope of the surrounding earth pressure calculation method that is based on the PPAT. Moreover, they have reference value for designing underground space structures.

2. Revisiting PPAT

2.1. Arch Stability Requirements

In the PPAT, it is assumed that an arch is rigid with an unlimited strength. In practice, the arch is made up of rock or soil materials with a limited strength. The arch material may undergo strength failure under a high axial force. The material damage can be analyzed in the stress space; however, what is obtained from the PPAT is the axial force instead of the stress. Although Niu et al. [20] put forward three conditions for a stable arch, it is difficult to judge whether the arch material is in a yielding state or not based on the magnitude of the force. To solve this problem, Zhang et al. [23] calculated the stress in the arch by assuming the arch thickness without providing a method to determine the thickness, making it difficult to use the proposed criterion. Note that the internal force of the arch is only the axial force; it can be considered that the arch material is in a state of uniaxial stress. As long as the axial stress in the arch is lower than the uniaxial compressive strength of the material, the arch will not undergo strength failure. Because the axial stress direction in the arch is tangent to the arch equation, the axial stress in the arch can be considered the tangential stress. If the tangential stress of the arch can be determined, the strength criterion that the arch material needs to meet can be established.

The PPAT does not fully consider the arch foot stability. When Protodyakonov determined the magnitude of the horizontal force at the arch foot, the author believed that the arch foot was prone to horizontal displacement and changed the internal force of the entire arch, which means that the arch foot would slide into the rock or soil mass in the horizontal direction. However, in practice, the stability of the entire arch depends on the bearing capacity of the rock or soil at the arch foot. Since the failure plane due to sliding at the arch foot has been assumed to form an angle of $45^\circ - \frac{\varphi}{2}$ with the side wall of the cave, the most likely mode for arch foot instability is sliding to the cave along the assumed failure plane, as indicated by the red dashed line in figure 1. Therefore, the second requirement for forming a stable NBA is that the arch foot should not slip along the failure plane.

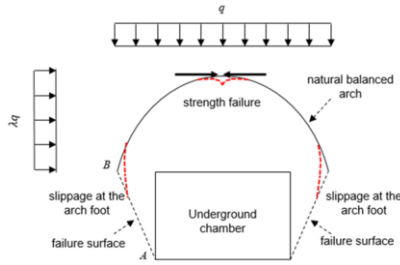


Figure 1. Potential failure mode of a naturally balanced arch.

2.2. Assumptions of modified PPAT (M-PPAT)

Some necessary assumptions are required to establish a new arch equation considering the stability of the arch foot. Nevertheless, based on the assumptions of the PPAT, an arch material is a type of loose rock or soil medium with little cohesiveness. The rock or soil mass at the roof of the cave will form an NBA after excavation. Two failure planes with an angle of $45^\circ - \frac{\varphi}{2}$ with respect to the side wall of the cave are formed. A uniform vertical strata pressure q acts on the top of the arch, and a uniform horizontal earth pressure of λq acts on the side of the arch, as illustrated in figure 2. The lateral pressure coefficient λ is assumed to be $0 < \lambda \leq 1$. Under the action of the external force, the internal force of the arch is only the axial force without bending moment or shear force.

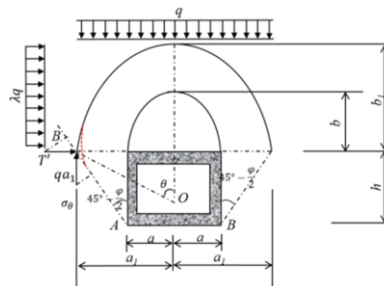


Figure 2. Schematic of the decomposition of the force at arch foot.

Assuming that the arch foot bears the thrust T' in the horizontal direction, the condition for the arch foot not to slide is that the decomposition of the supporting reaction force qa_1 along the failure surface is less than the decomposition of T' along the failure surface, as indicated by the red dashed line in figure 2. T' can be given based on the reaction vertical force, without considering the hardness coefficient of the soil, which is difficult to determine.

Evidently, the main difference between the new theory and the classical PPAT is that the arch foot stability and the side pressure are considered. For the arch obtained under the new hypothesis, the arch foot is ensured to be in a stable state. The arch equation considering the side pressure is not novel. Some scholars [35] have considered it; however, the stability of the arch foot was not considered.

2.3. M-PPAT

The NBA axis is assumed to be a curve. Half of the curve is taken as the analysis object. The curve is subjected to a vertical uniform load q and a horizontal uniform load λq . The cross section at the top of the curve is subjected to an internal force T in the horizontal direction. The arch foot is subjected to a horizontal force T' and a vertical reaction force qa_1 . The height of the arch is b_1 , and the half span of the arch is a_1 . The above assumptions are illustrated in the analysis diagram shown in figure 3.

Since there is no bending moment of the arch, taking any point $M(x, y)$ on the arch as the analysis object, the moment at any position on the arch relative to this point is 0.

Thus,

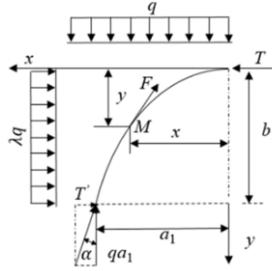


Figure 3. Analysis model of M-PPAT.

$$Ty = \frac{1}{2}qx^2 + \frac{1}{2}\lambda qy^2 \quad (1)$$

Based on the horizontal force balance, an equilibrium equation can be obtained.

$$T = T' + \lambda qb_1 \quad (2)$$

If the arch is to be stable, it is necessary to prevent the arch foot from slipping off along the assumed failure plane. Thus,

$$T' \sin\left(45^\circ - \frac{\varphi}{2}\right) \leq qa_1 \cos\left(45^\circ - \frac{\varphi}{2}\right) \quad (3)$$

That is,

$$T' \leq qa_1 \cot\left(45^\circ - \frac{\varphi}{2}\right) \quad (4)$$

For safety,

$$T' = \frac{1}{2}qa_1 \cot\left(45^\circ - \frac{\varphi}{2}\right) \quad (5)$$

Substituting Equation (5) into Equations (1) and (2) and subtracting q yield the following:

$$x^2 + \lambda y^2 - \left(a_1 \cot\left(45^\circ - \frac{\varphi}{2}\right) + 2\lambda b_1\right)y = 0 \quad (6)$$

This is the modified arch equation considering the lateral pressure and the stability of the arch foot. The equation represents an ellipse. The ratio of the major axis to the minor axis of this ellipse is $\sqrt{\lambda}$; in other words, the shape of the arch formed under the action of the external force is determined; however, the size varies with the parameters of the cave and surrounding rock.

Based on the assumptions made previously, the angle between the failure plane and the side wall is $45^\circ - \frac{\varphi}{2}$, and a_1 is given by the following formula:

$$a_1 = a + h \tan\left(45^\circ - \frac{\varphi}{2}\right) \quad (7)$$

Here, a is the half span of the cave, h is the height of the cave, and φ is the friction angle of the surrounding rock. Substituting $x = a_1$ and $y = b_1$ into Equation (6) yields:

$$b_1 = \frac{(a+h \tan(45^\circ-\frac{\varphi}{2})) \cdot (\sqrt{4\lambda + \cot^2(45^\circ-\frac{\varphi}{2})} - \cot(45^\circ-\frac{\varphi}{2}))}{2\lambda} \quad (8)$$

For the convenience of a comparative analysis, assuming the horizontal thrust T' of the arch foot satisfies the equation $T' = \frac{1}{2}qa_1f$, the arch equation that considers the lateral pressure but does not consider the arch foot stability can be obtained as follows.

$$x^2 + \lambda y^2 - (a_1f + 2\lambda b_1)y = 0 \quad (9)$$

Equation (9) is also an ellipse. The arch height can be given as:

$$b_1 = \frac{(a+h \tan(45^\circ-\frac{\varphi}{2})) \cdot (\sqrt{4\lambda + f^2} - f)}{2\lambda} \quad (10)$$

The ratio of the long axis to the short axis of Equation (10) is still $\sqrt{\lambda}$. For the convenience of expression, the arch equation represented by formula (9) can be simply called L-PPAT.

3. Stability Criterion of NBA

3.1. Arch Strength Criterion

The internal force of the arch line can be calculated from the arch equation. However, to assess whether the arch is damaged or not under the action of the axial force, the force analysis of the arch should be converted to the strength analysis of the arch material. Since the shape of the NBA is a stable ellipse overall, the rock or soil surrounded by the arch ring is a loose medium, and ignoring the influence of gravity, the internal force of the arch can be approximated based on the stress distribution of an elliptical cave. The stable arch material should meet the strength requirements; therefore, it can be considered that the arch is in an elastic stress state, and the stress distribution of the elliptical cave can be obtained using the linear elastic solution. Under the stress conditions shown in figure 3, only the tangential stress component σ_θ at the wall of the elliptical cave is not 0; thus, the tangential stress σ_θ can be approximately equal to the internal pressure stress of the arch. Therefore, the arch strength criterion can be established by checking whether the arch internal stress meets the material strength requirements.

The tangential stress component σ_θ of the elliptical cave [36] can be expressed as follows:

$$\sigma_\theta = \frac{q[(1+m)^2 \sin^2 \theta - m^2 + \lambda(1+m)^2 \cos^2 \theta - \lambda]}{\sin^2 \theta + m^2 \cos^2 \theta} \quad (11)$$

Here, q is the vertical earth pressure acting above the arch, $m = \frac{s}{l} = \sqrt{\lambda}$, s is the minor axis of the elliptic curve, and l is its major axis. Substituting m into Equation (11) yields:

$$\sigma_\theta = q(1 + \sqrt{\lambda})^2 - \frac{2q\lambda}{\sin^2 \theta + \lambda \cos^2 \theta} \quad (12)$$

Based on the results of the previous analysis, the tangential stress of the surrounding rock at the top of the arch should be lower than the uniaxial compressive strength of the rock mass. Thus,

$$\sigma_\theta \leq R_b \cdot K_v \quad (13)$$

where R_b is the standard value of the uniaxial compressive strength of the rock block in laboratory tests, and K_v is the rock mass integrity coefficient, which is equal to the longitudinal wave velocity of the rock mass divided by the longitudinal wave velocity of the rock blocks. As the lateral pressure coefficient λ is assumed to be $0 < \lambda \leq 1$, when $\theta = 0$, the tangential stress of the elliptical cave is the highest from Equation (12). The materials at the top of the arch are the first to fail. Substituting $\theta = 0$ into Equation (12), Equation (13) becomes:

$$q \left((\sqrt{\lambda} + 1)^2 - 2 \right) \leq R_b \cdot K_v \quad (14)$$

Equation (14) is the strength criterion of a stable rock arch. Let $q = \gamma H_a$, γ is the equivalent weight of the overlying strata, and H_a is the buried depth of the arch. Substituting it into Equation (14) yields:

$$H_a \leq \frac{R_b \cdot K_v}{\gamma((\sqrt{\lambda} + 1)^2 - 2)} \quad (15)$$

This is the burial depth limitation for arching in rock formations. For soil formations, $R_b \cdot K_v$ in Equation (15) is substituted with the unconfined uniaxial compressive strength of the soil material, q_u , namely

$$H_a \leq \frac{q_u}{\gamma((\sqrt{\lambda} + 1)^2 - 2)} \quad (16)$$

This is the buried depth limitation for a stable soil arch.

3.2. Arch Foot Stability Criterion

In addition to the insufficient material strength threatening the stability of a balanced arch, the slippage of the arch foot along the assumed failure plane is another reason for the arch instability. Suppose the force of the arch on the rock mass at the arch foot is F and the comprehensive friction coefficient on the failure plane is μ , a stable arch foot should satisfy:

$$\mu F \sin \left(45^\circ - \frac{\varphi}{2} + \alpha \right) \geq F \cos \left(45^\circ - \frac{\varphi}{2} + \alpha \right) \quad (17)$$

The force F on both sides of Equation (17) is eliminated, without considering the cohesion effect, then, $\mu = \tan \varphi$, and,

$$\tan \left(45^\circ - \frac{\varphi}{2} + \alpha \right) \cdot \tan \varphi \geq 1 \quad (18)$$

where φ is the internal friction angle of the surrounding rock, and α is the angle between the force at the arch foot and the vertical line. As the horizontal reaction force at the arch foot is determined by Equation (5) and combined with the vertical reaction force being qa_1 , the following can be written:

$$\alpha = 90^\circ - \tan^{-1} \left(\frac{1}{2} \cot \left(45^\circ - \frac{\varphi}{2} \right) \right) \quad (19)$$

Equation (17) is the criterion for the stability of the arch foot, which is a sufficient criterion for arching. When $\mu = \tan \varphi$, the equation is only suitable for sandy soils. For a cohesive stratum, the calculated internal friction angle φ_k should be used instead of the internal friction angle φ . Arches with assumptions that do not satisfy Equation (18) will be unstable and will collapse along the failure plane.

4. Verification

Currently, the experiment used to study the natural arching of granular materials is mainly the trapdoor test. Terzaghi [9] first conducted this experiment and revealed the process and regular pattern of the formation of a stable NBA. Many follow-up studies [37–46] were conducted to further explore the arching mechanism of granular materials through this experiment and discrete element methods. Therefore, the trapdoor experiment combined with the PFC2D numerical simulation can be used to verify the rationality of the revisited method proposed in this article.

4.1. Trapdoor Test

4.1.1. Test Apparatus

The test apparatus is mainly composed of structural plates, plexiglass, and anchor bolts (see figure 4). The plexiglass and structural plates are kept hollow. The thickness of the hollow part is approximately 20 mm, the height is 700 mm, and the width is 500 mm. Different granular materials can be filled. The plexiglass is 12 mm thick and has a strong lateral rigidity to ensure that the amount of compression deformation during the test is negligible. Different from the vertical outlet design of the classical trapdoor test apparatus, the bottom outlet is designed as an inverted trapezoid. The width of the lower outlet of the trapezoid is 40 mm, and the width of the upper outlet is 145 mm. The angle α between the trapezoidal inclined plane and the horizontal plane is approximately 60° . This design is mainly to simulate the failure process of the NBA along the failure plane as aforementioned.

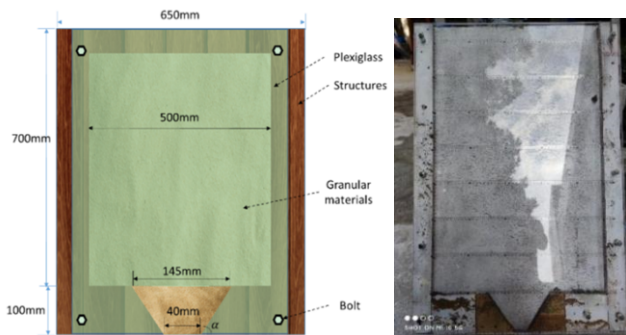


Figure 4. Trapdoor apparatus.

4.1.2. Granular Materials and Test Process

Pea stones are used as test granular materials. Table 1 presents the characteristics of the particles with different sizes. Figure 5 shows the gradation curve of the pea stones. The friction angle, static lateral pressure coefficient, and hardness coefficient of the pea stones are taken as the parameters of the coarse-grained soil, as listed in table 2. From tables 1 and 2, the diameters of the pea granite particles are mainly distributed in the ranges of 5–8 mm and 8–12 mm, accounting for 43.7% and 42.9%, respectively. During the test, the first step is to seal the lower exit of the trapdoor with a transparent glue and then fill pea stones to a predetermined height of 250 mm. Subsequently, the

test apparatus is erected. After the preparation work is completed, the transparent glue at the exit of the trapdoor is carefully torn off, so that the pea stones at the exit are suspended and fall freely. A stable arch, as shown in Figure 6, can be formed until the pea stones above the arch no longer fall.

Table 1. Characteristics of pea stones with different sizes.





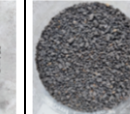
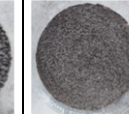
Particle size(mm)	>12	8-12	5-8	3.5-5	1.0-3.5	<1.0
Image						

Table 2. Parameters of pea stones.

Cohesion(kPa)	Friction angle $\varphi(^{\circ})$	Static lateral pressure coefficient	Hardness coefficient of f
0	42	0.4	2.0

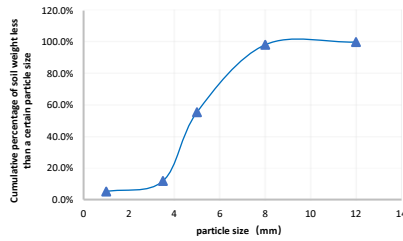


Figure 5. Gradation curves of pea stones.

Figure 6. Pea stone trapdoor test arching diagram.

4.1.3. Test Results

A stable NBA is formed in this trapdoor experiment (figure 6). The arch foot fell on an inverted trapezoid slope. The left foot arch crossed the slope at approximately 92° , and the right foot arch crossed the slope at approximately 85° . The position of the right arch is slightly higher than that of the left arch, and the upper arch axis is approximately arc-shaped. The measured arch span $2a_1$ is 56 mm, and the arch height b_1 is 12 mm.

4.2. PFC2D Simulation

To further explore the arching mechanism of granular materials in the trapdoor experiment, PFC2D is used to simulate the test process. The PFC2D is a discrete element simulation product developed by ITASCA, which is based on the granular material simulation method proposed by Cundall et al. [47]. The software has been proved to be a good numerical tool for simulating the mechanical behavior of granular materials.

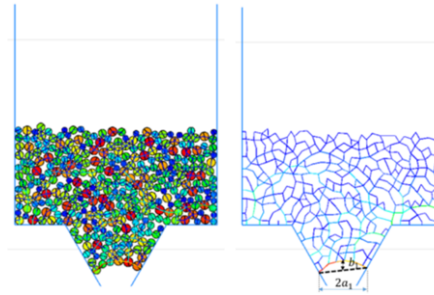
The linear contact model is used to simulate the ball-to-ball contact and the ball-to-surface contact. According to the results of the gradation test, the grain size of 3.5mm or more of the pea stones used in the trapdoor test accounts for more than 95%, so the simulated particle size is set between 3.5~12mm, and the particle spheres are generated according to the gradation curve in figure 5. Table 3 presents the model parameters.

The initial height of the covering layer is consistent with the initial height employed in the trapdoor test. The model exit is still an inverted trapezoid.

Table 3. Input parameters for PFC2D simulation.

Model type	Model	Normal stiffness k_n (Pa)	Shear stiffness k_s (Pa)	Friction	Normal critical damping ratio
Ball-ball contact model	Linear	1e8	1e8	1.0	0.8
ball-facet contact model	Linear	1e10	1e10	0.3	0.8

The simulation results show that the falling of the granular material forms a stable NBA, as shown in figure 7. The arch feet of the NBA on both sides simulated by PFC2D cross the inclined plane at approximately 90° , the right arch foot is slightly higher than the left arch foot, and the force chain between the particles of the arch forms a typical arch. This is similar to the trapdoor test results.



(a) Contact force distribution between balls (b) Arch of the force chain

Figure 7. PFC2D simulation of the naturally balanced arching phenomenon.

4.3. Comparative Analysis

To verify the rationality of M-PPAT, the trapdoor test results were used to calculate the arch heights by PPAT, L-PPAT, and M-PPAT respectively. Among them, PPAT arch height is calculated by formula (20), L-PPAT arch height is calculated by formula (10), and M-PPAT arch height is calculated by formula (8).

$$b_1 = \frac{a_1}{f} \quad (20)$$

In the formula(8), (10) and (20), a_1 takes the measured value of the trapdoor test, f is the hardness coefficient of pea stones and equals 2, the friction angle φ is taken from table 2. The calculation results of each method (including the height of NBA formed by PFC simulation) are listed in table 4, and the error between each method and the test result is given.

Table 4. Comparison of measured, simulated and calculated results.

Method	PPAT	L-PPAT	M-PPAT	Trapdoor test	PFC2D
Arch height b_1 (mm)	14.0	12.8	11.6	12.0	9.5
Error	16.7%	6.9%	3.3%	0%	20.8%

It can be seen from table 4 that the differences between the calculated results of PPAT, L-PPAT and M-PPAT and the trapdoor test results are 16.7%, 6.6%, and 3.3%, respectively. This result shows that when the lateral stress is not considered, the calculated arch height will greatly deviate from the actual arch height that can be formed by the granular material. The M-PPAT, which considers the lateral stress and the stability of the arch foot at the same time, is closer to the measured value of the trapdoor test than the L-PPAT which only considers the lateral stress.

The results of the PFC2D simulation are quite different from the measured values in the experiment. This is not only because the numerical simulation results depend on the input parameters, but also because the particles in PFC2D are round particles, which are quite different from the shape of the pea stones. The equivalent relationship between the two has not been found. But the PFC2D simulation result can still show that the granular material could form a stable NBA, but the arch height it could form is very limited, unlike the PPAT reveals.

5. Discussion

5.1. Arch Height and Stability

To illustrate the application of the revisited arch equation and arching criterion in the design, the following examples are taken: typical silty clay, clay, dry compacted sand, strongly weathered mudstone, moderately weathered sandstone, and moderately weathered limestone formations. Table 5 lists the parameters. Assuming that each stratum is a single uniform stratum, in which a cave with a span of 6 m and a height of 6 m is excavated, the arch height of each theoretical hypothesis is calculated using the aforementioned theoretical formula, and each arch is judged on the basis of the stability criterion of the arch foot. Table 6 presents the results.

Table 5. Case parameters.

strata type	λ	γ (kN/m ³)	a (m)	h (m)	f	φ (°)
silty clay	0.6	18.5	3	6	0.5	20
clay	0.55	19	3	6	1	20
dry compacted sand	0.58	19	3	6	0.8	25
strongly weathered mudstone	0.45	26	3	6	2	40
moderately weathered sandstone	0.35	26	3	6	4	42
moderately weathered limestone	0.43	24	3	6	6	45

In various soil formations, the arch height of the PPAT is much higher than those of L-PPAT and M-PPAT. Except for M-PPAT, neither PPAT nor L-PPAT meet the requirements of arch foot stability. Although the arch heights calculated by PPAT and L-PPAT are greater than that calculated by M-PPAT, they are not balanced arches and cannot fully bear the upper stratum pressure like a real NBA. This means that the height of the NBA is limited by the arch foot stability criterion in soil formations.

However, an arch that is too low cannot ensure the stability of the arch foot. In moderately weathered limestone formations, as listed in table 6, PPAT and L-PPAT have a lower arch height than M-PPAT, but their arch foot is unstable. For rock formations, the PPAT may underestimate the arch height, even if the lateral pressure is

considered. The revisited arch can give a reasonable arch shape that meets the arch foot stability requirements.

Some scholars and codes aforementioned [1-3,34,35] use empirical formulae to calculate the arch height based on the classification of the surrounding rock. The arch height calculated by these formulae is often greater than the theoretical calculation result. Taking the strongly weathered mudstone formation in table 5 as an example, according to China's surrounding rock grading standards [48], the surrounding rock grading to which it belongs is generally Grade V. The arch height is given [1-3] by

$$b_1 = 0.45 \times 2^{S-1}w \quad (21)$$

where S is the surrounding rock grade, w is the cave span influence coefficient, and b_1 is the height of the arch. Substituting $S = 5$ and $w = 1.1$ into Equation (21), we can obtain $b_1 = 7.04$ m, which is much greater than those of PPAT, L-PPAT, and M-PPAT. Although the higher arch height seems to have a larger safety factor, the theoretical basis of the calculation result is unreliable. In particular, when the failure mode of the cave is squeezing large deformation, a stable natural equilibrium arch cannot be formed, and the surrounding rock pressure should be calculated using the convergence-constraint theory [49].

Table 6. Calculation results.

strata type	PPAT		L-PPAT		M-PPAT	
	b_1 (m)	Arch foot stability	b_1 (m)	Arch foot stability	b_1 (m)	Arch foot stability
silty clay	14.4	unstable	6.8	unstable	4.1	stable
clay	7.2	unstable	5.3	unstable	4.2	stable
dry compacted sand	8.5	unstable	5.4	unstable	3.6	stable
strongly weathered mudstone	2.9	stable	2.6	stable	2.5	stable
moderately weathered sandstone	1.4	stable	1.4	stable	2.4	stable
moderately weathered limestone	1.4	unstable	1.4	unstable	3.3	stable

5.2. Maximum Arching Depth

The maximum arching depth can be given by Equations (15) and (16). Taking silty clay as an example, the maximum arching depths considering different λ values and uniaxial compressive strengths in the silty clay formation are plotted in figure 8. The greater the λ value, the lower the maximum arching depth, and the weaker the surrounding rock, the lower the maximum arching depth. Once the maximum arching depth limit is exceeded, this type of soil cannot form a stable NBA. In addition, water has an important influence on the soil strength; therefore, the arching judgment of the water-rich stratum should be more conservative.

The same regular pattern also exists in rock formations. Taking mudstone as an example, the maximum arching depths considering different λ and uniaxial compressive strengths in the mudstone formation are plotted in figure 9. The arching ability is limited by the buried depth in soft rock formations with large buried depth and high lateral pressure coefficient. This means that the applicable range of the surrounding earth pressure calculation method based on the PPAT should be strictly limited, particularly for V-level surrounding rock formations according to the BQ ranking theory used in China [48].

5.3. Applicability of M-PPAT

M-PPAT does not consider the cohesion effect of soil like PPAT. But in fact, soil cohesion is conducive to form a stable arch. Therefore, the M-PPAT proposed in this paper should not be used to calculate the arch height in cohesive formation, but the arching criterion of a stable NBA should satisfy is still applicable in such formation.

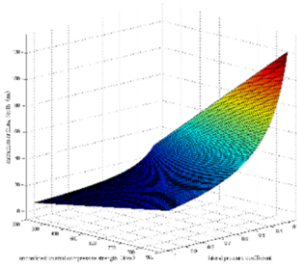


Figure 8. Maximum arching depths in silty clay formation.

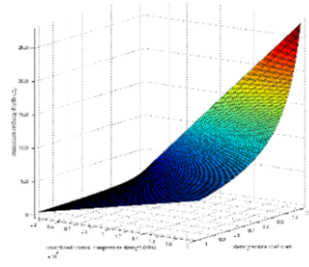


Figure 9. Maximum arching depths in mudstone formation.

6. Conclusions

This study mainly improved the PPAT and established a stability criterion for the NBA. The following conclusions can be drawn:

(1) A stable NBA not only requires an axial pressure in the arch without bending moments or shear stress, but also requires the arch materials to meet the strength criterion and the arch foot to be in a stable state. Considering the lateral stress and arch foot stability, an improved arch axis equation M-PPAT was established. Expressions for the arch strength criterion and arch foot stability criterion were provided.

(2) The results of trapdoor test and PFC2D simulation showed that the difference between the arch height calculated by M-PPAT and the trapdoor test result is only 3.3%, which is much better than the height given by PPAT. The particle flow simulation results for the trapdoor test by PFC2D show that the particle material can form a stable NBA, and the shape of the arch is very close to the test results.

(3) The arch foot stability criterion was used to test the stability of the arches formed in the soil using the arch axis equation, which does not consider the arch foot stability, and it was found that these arches are unstable except for M-PPAT. The arch foot stability criterion limits the arch height of stable NBA in soil formations. However, in some rock formations, the arch height obtained using the revisited arch axis equation was higher, indicating that the arch foot stability criterion can avoid excessively low arch height in such types of rock formations.

(4) The maximum buried depth for stable NBA formation was found to be limited by the arch strength criterion. The greater the strength, the deeper the maximum arching depth. A stable NBA cannot be formed for buried depths exceeded the limit. Since M-PPAT does not consider cohesion, this theory should be used with caution in cohesive soil formations.

Notably, a stable NBA cannot be formed for certain depths based on the arch strength criterion, but it should not be assumed that the arching effect does not exist. On the other hand, the arch effect is also limited by the shallowest buried depth [50].

When using the criterion proposed in this article, the shallowest buried depth limit should be considered.

Acknowledgements

This work is supported by the Key R&D Program of Hubei NO.2022BCA080, and the National Key R&D Program of China (2019YFC0605103, 2019YFC0605104). Grateful acknowledgement is made to Professor Li Chunguang and Lin Songqing who gave me considerable help by means of suggestion, comments and criticism. I also thank Liu Zhongbo from Wuhan University of Technology, who helped me complete part of the trapdoor experiments.

The authors declare that they have no conflicts of interest.

References

- [1] China Railway Eryuan Engineering Group Co.Ltd, 2017. TB10003-2016 Code for Design of Railway Tunnel. China Railway Press Co., Ltd, Beijing, pp. 131-132.
- [2] China Merchants Chongqing Communications Technology Research & Design Institute Co., Ltd ,2019. JTG 3370.1-2018 Specification for Design of Highway Tunnels Section 1 Civil Engineering. China Communications Press Co., Ltd, Beijing, pp. 33-34.
- [3] Beijing Municipal Commission of Planning and Natural Resources, 2013. GB50157-2013 Code for Design of Metro. China Architecture Publication & Media Co., Ltd, Beijing, p.87.
- [4] Taghizadeh H, Zare S, Mazraehli M. Analysis of rock load for tunnel lining design. *Geotech. Geol. Eng.* 2020; 38(5), 2989–3005.
- [5] Deere DU, Peck RB, Monsees JE, et al. Design of tunnel liners and support systems: final report. Highway Research Record 339, US Department of Transportation, Washington DC, 1969; pp. 41-45.
- [6] Singh B, Viladkar MN, Samadhiya NK. A semi-empirical method for the design of support systems in underground openings. *Tunn. Undergr. Space Technol.* 1995; 10(3), 375-383.
- [7] Moradi G, Abbasnejad A. The state of the art report on arching effect. *Journal of Civil Engineering Research.* 2013; 3(5): 148-161.
- [8] Wang M. Tunneling and Underground Engineering Technology in China. China Communications Press, Beijing, 2010; pp. 55-65.
- [9] Terzaghi KT. *Theoretical Soil Mechanics*. Wiley, New York, 1943; pp. 66-76.
- [10] Handy RL. The arch in soil arching. *J. Geotech. Eng.* 1985; 111(3): 302-318.
- [11] Kingsley HW. Arch in soil arching. *J. Geotech. Eng.* 1989; 115(3): 415-419.
- [12] Hall CD, Harrisberger WH. Stability of sand arches: a key to sand control. *J. Pet. Technol.* 1970; 22(07), 821-829.
- [13] Guo PJ., Zhou SH, et al. Arch in granular materials as a free surface problem. *Int. J. Numer. Anal. Methods Geomech.* 2012; 37(9): 1048-1065.
- [14] Xu D, Zhou SH, et al. Discussion about the arching capacity of Shanghai clay. *Journal of Shanghai Tiedao University (Natural Science Edition).* 1999; 20(6): 49-54.
- [15] Liang XD, Liu G, Zhao J. Definition and analysis of arching action in underground rock engineering. *Journal of Hehai University (Natural Sciences).* 2005; (03): 314-317.
- [16] Liang X. Experimental and numerical analysis on the arching action from stress adjusting in surrounding rocks. *Journal of Engineering Geology.* 2012; 20(01): 96-102.
- [17] Wang S, Hagan P, Cheng Y, et al. Experimental research on fracture hinged arching process and instability characteristics for rock plates. *Chin. J. Rock Mech. Eng.* 2012; 31(8): 1674-1679.
- [18] Jia J, Zhou SH, Gong QM. Stress release characteristics of sandy soil arching by laboratory tests and numerical simulation. *Rock Soil Mech.* 2013; 34(2), 395-403.
- [19] Li TF, Chen QN, Ma XP, et al. The minimum buried depth of soil tunnel natural form arch based on twin shear strength theory. *Journal of Hunan Institute of Engineering.* 2013; 23(03): 78-80.
- [20] Niu X, Ding X. Bearing mechanism of top arch and stable arch design method for surrounding rock of underground caverns. *Chin. J. Rock Mech. Eng.* 2013; 32(4): 775-786.
- [21] Yang JH, Wang SR, Wang YG, et al Analysis of arching mechanism and evolution characteristics of tunnel pressure arch. *Jordan Journal of Civil Engineering.* 2015; 9(1): 125-132.

- [22] Zheng YR, Qiu C. On the limitations of Protodyakonov's pressure arch theory. *Modern Tunneling Technology*. 2016; 2: 1-8.
- [23] Erdi A, Zheng YR, Feng XT, et al. Analysis of circular tunnel stability based on the limit strain method. *Appl. Math. Mech* 2015; 36(12): 1265-1273.
- [24] Su YH, He XL, Luo ZD. Research on stability of tunnel surrounding rock based on strength reduction method. *Hydrol. Eng. Geol.* 2014; 41(01): 48-53.
- [25] Li N, Chen Y, Chen F, et al. Research on tunnel stability criterion. *Chin. J. Rock Mech. Eng.* 2006; 25(9): 1941-1944.
- [26] Li N, Liu N, LI GF. New method for stability evaluation of soil and soft rock tunnels. *Chin. J. Rock Mech. Eng.* 2014; 33(09): 1812-1821.
- [27] Zhu WS, Sun AH, Wang WT, et al. Study on prediction of high wall displacement and stability judging method of surrounding rock for large cavern groups. *Chin. J. Rock Mech. Eng.* 2007; 09: 1729-1736.
- [28] Sun ZY, Zhang DL, Hou YJ, et al. Whole-process deformation laws and determination of stability criterion of surrounding rock of tunnels based on statistics of field measured data. *Chin. J. Geotech. Eng.* 2021; 43(07): 1261-1270.
- [29] Li XH, Wang HT, Jia JQ, et al. Ultimate displacement discrimination of stability and reliability analysis of surrounding rocks of tunnel and underground engineering. *Rock Soil Mech.* 2005; 26(6): 850-854.
- [30] Dong Y, Zhang MS, Li N, et al. Methods and contents of geological safety evaluation for urban underground space development and utilization. *Hydrol. Eng. Geol.* 2020; 47(05): 161-168.
- [31] Gong FQ, Li XB. The Bayes discriminant analysis method for stability evaluation of rock surrounding in tunnel and its application. *Chin. J. Undergr. Space Eng.* 2007; (06): 1138-1141.
- [32] Xu F, Xu WY, Wen S, et al. Projection pursuit based on particle swarm optimization for evaluation of surrounding rock stability. *Rock Soil Mech.* 2010; 31(11): 3651-3655.
- [33] Sun J. Study and application on key technology of tunnel structure design. China Communications Press Co., Ltd, Beijing, 2014; pp. 35-37.
- [34] Barton N, Lien R, Lunde J. Engineering classification of rock masses for the design of tunnel support. *Rock Mech. Rock Eng.* 1974; 6(4): 189-236.
- [35] Lowson AR & Bieniawski ZT. Critical assessment of RMR-based tunnel design practices: A practical engineer's approach. *Proceedings, Rapid Excavation & Tunneling Conference*. 2013; pp. 180-198.
- [36] Gao XL. A general solution of an infinite elastic plate with an elliptic hole under biaxial loading. *Int. J. Pressure Vessels Piping*. 1996; 67(1): 95-104.
- [37] To K, Lai PY, Park HK. Jamming pattern in a two-dimensional hopper. *Phys. Rev. E*, 2001; 86(1): 71-74.
- [38] Ahmadi A, Hosseininia ES, et al. An experimental investigation on stable arch formation in cohesionless granular materials using developed trapdoor test. *Powder Technol.* 2018; 330: 137-146.
- [39] Jung YH, Kim TG, Sim D, et al. Investigating the origin of the soil arch in the trapdoor problem: photoelastic measurement and discrete element simulation. *Proceedings, International Conference on Discrete Element Methods*, 2017; pp. 1039-1045.
- [40] Jiang MJ, Du WH, Xi BL., Distinct element numerical simulation of trapdoor tests for pure and cemented sands. *J. Earth Sci. Environ.* 2018; 40(3): 347-354.
- [41] Takashi, SUGIYAMA, Mikio, et al. Applicability of the distinct element method to investigation by the trap door test using sandy soil. *Proceedings of Tunnel Engineering, JSCE*. 1993; 3: 25-32.
- [42] Toshio, Noguchi, Hisashi, et al, 1996. Study on vertical earth pressure distribution in sand by trap door test. *Doboku Gakkai Ronbunshu*. 1996; 534: 77-85.
- [43] Noguchi T, Tarumi H. Study on vertical earth pressure distribution in sand by trap door test. *Proceedings of the Japan Society of Civil Engineers*. 2010; 534: 77-85.
- [44] Sugimoto S, Ochiai H, Yasufuku N, et al. Development of stress measurement system and its application for evaluating mechanical behavior of trap door test. *Doboku Gakkai Ronbunshu*. 2011; 15: 211-216.
- [45] Bi Z, Gong Q, Guo P, et al. Experimental study of the evolution of soil arching effect under cyclic loading based on trapdoor test and particle image velocimetry. *Can. Geotech. J.* 2020; 57(6): 903-920.
- [46] Park KH, Baek SH, Jung YH. Investigation of arch structure of granular assembly in the trapdoor test using digital RGB photoelastic analysis. *Powder Technol.* 2020; 366: 560-570.
- [47] Cundall PA, Strack O. A discrete numerical model for granular assemblies. *Geotechnique*. 2008; 30(3): 331-336.
- [48] Ministry of Water Resources of the People's Republic of China. GB/T 50218-2014 Standard for engineering classification of rock mass, China Planning Press, Beijing, 2014; pp. 4-9.
- [49] Hoek E. Big tunnels in bad rock. *J. Geotech. Geoenviron. Eng.* 127(9), 726-740.
- [50] Zhang P, Lu D, Du X, et al. A division method for shallow tunnels and deep tunnels considering soil stress path dependency. *Computers and Geotechnics*. 2001; 135: 1-14.